One- and two-photon double ionization of beryllium with ultrashort ultraviolet laser fields

S. Laulan* and H. Bachau

Centre Lasers Intenses et Applications, UMR 5107 du CNRS-CEA-Université Bordeaux I, Université de Bordeaux I,
351 Cours de la Libération, F-33405 Talence, France
(Received 7 October 2003; published 23 March 2004)

The interaction between the beryllium atom and short laser fields is treated on the basis of the nonrelativistic time-dependent Schrödinger equation. We calculate total cross sections and electron energy distributions for the double ionization of the valence electrons through one- and two-photon absorption. We introduce a model potential to represent the $1s^2$ core. The emphasis is put on the double ionization of the valence electrons in the context of ultrashort pulses. Results will be also presented for the ionization of the inner electrons.

I. INTRODUCTION

With the emergence of new free-electron laser (FEL) sources, it will be soon possible to explore light-matter interactions with high frequency fields at high intensity and short pulse durations [1–3]. The increasing efficiency of the generation of high-order harmonics is also a promising short wavelength light source [4]. This opens the way to study nonlinear processes with short wavelengths at the time scale of electronic correlations. A recent example of application of harmonics is the experimental and theoretical study of two-photon ionization of He with harmonics of the Ti:sapphire laser [5]. The development of these new sources has led the theoretical community to investigate multielectronic processes in the nonlinear regime. In particular, recent studies have concentrated on the double photoionization of two active electron atomic systems in the UV regime, with more than one photon absorbed. Much attention has been paid to the electron energy distribution, which is directly related to the ionization mechanism (direct or sequential). A large literature already exists for the helium atom (see Ref. [6], denoted as paper I in the following, and other references therein) but the case of more complex systems has received less attention. We note the recent work on two-photon double ionization of magnesium [7]. The double and triple ionization of beryllium has been also recently studied, from both the theoretical and experimental sides, but in the context of one-photon absorption [8–12].

We showed in paper I that the relative magnitude of the pulse duration and correlation time in the initial atomic state plays a crucial role in the electron spectrum produced by the two-photon double electron ejection of He. This has led us to explore similar processes in alkaline-earth atoms. It is easier to double ionize the valence electrons in these systems because the time scale of the correlations in the uppermost shell is closer to the femtosecond regime. For example, in beryllium, two-photon ionization requires about 13.7 eV photons, the electron interaction energy of the $2s^2$ state being about 8.4 eV (0.49 fs). These latter numbers have to be compared to 79 and 30 eV (0.14 fs), respectively, in helium.

Therefore, it should be easier to perform experiments involving atoms with a multielectronic core. From the theoretical point of view, it is still a challenging problem to represent the double continuum in complex atoms, and the presence of the core places additional demands on the calculations.

In this paper, we extend our theoretical method to the study of the one- and two-photon double ionization of the beryllium atom. Besides the absolute cross sections for double ionization, the electron energy distribution spectrum is of great interest and it has to be determined. We have shown that, in two-photon double ionization with long pulse duration, the sequential regime is favored when it is energetically allowed, which results in two peaks in the electron energy distribution [13]. In the regime of ultrashort interactions (femto- or subfemtoseconds), the time scale of electronic correlations in the atomic ground state is reached and the electron energy spectrum tends to a single peak. The reason for such behavior is that, once one photon has been absorbed, the relaxation of the parent ion has no time to occur before the second photon is absorbed [14]. These effects have been thoroughly studied in helium (see paper I for references). The aim of this work is to extend our investigations to the case of the Be atom. We focus on the case of the ionization of the valence electrons, and, in a more prospective context, we also investigate the two-photon double ionization of the $1s^2$ core. Note that the two processes occur at very different wavelengths. On the one hand, the core ionization requires photon energies larger than 160 eV; at these wavelengths the ionization of the valence electrons plays a minor role. On the other hand, the double ionization of the $2s^2$ valence shell is investigated with photon energies of 14–20 eV. The multiphoton ionization of the core is negligible at the intensity considered in this work. We assume here that the relaxation of the outer (inner) electrons is neglected and consequently the photoionization process reduces to a two active electron problem. The "frozen" configuration $2s^2$ ($1s^2$) will be represented by a model potential. This type of approach has been extensively used for the photoionization of atomic systems (see Ref. [15] and references therein).

We develop the theoretical approach in the following section (it is of a spectral and configuration interaction type) and we solve the time-dependent Schrödinger equation (TDSE)

---

*Electronic address: laulan@celia.u-bordeaux.fr

for two active electron systems. Emphasis will be put on the description of the electronic structures in the presence of the model potentials. The correlations between the active electrons are fully included in the initial state and during the propagation. The numerical approach, based on B-splines, has been described in paper I and will not be developed here. In the applications we present first the ionization of Be($2s^2$). One-photon double ionization cross sections are calculated and compared with other theoretical calculations. Two-photon double ionization cross sections and electron distributions will be also calculated and discussed. Emphasis will be put on the evolution of the electron distributions with the pulse duration. Finally the case of the two-photon double ionization of the $1s^2$ core of Be will be investigated.

The calculations are performed at an intensity of 10^{14} W/cm², where three-photon absorption does not play a significant role. Atomic units are used throughout the paper unless otherwise mentioned.

II. THEORETICAL APPROACH

Our approach to resolve the TDSE has been described in detail in our previous works; therefore, it will be briefly presented here. Here we will endeavor to include the effect of the frozen configuration in our theory.

A. The two-active electron models

The electronic structure of the beryllium atom satisfies the equation

$$(H - E_n)\Psi_n = 0, \tag{1}$$

where H is the nonrelativistic Hamiltonian.

First, we investigate the case of the representation of the $2s^2$ valence shell of Be. The Hamiltonian reads

$$H = H_0(1) + V_M(1) + H_0(2) + V_M(2) + \frac{1}{r_{12}} + V_{ps}$$
$$= -\frac{1}{2}\Delta_1 - \frac{Z}{r_1} + V_M(1) - \frac{1}{2}\Delta_2 - \frac{Z}{r_2} + V_M(2) + \frac{1}{r_{12}} + V_{ps}, \tag{2}$$

where Z is the nuclear charge (here $Z=4$), and labels 1 and 2 refer to the two valence electrons. $V_M(i)$ is a model potential that describes the interaction between the $1s^2$ electronic core and the valence electron i:

$$V_M(i) = \frac{2}{r_i} - \frac{2}{r_i}(1 + \alpha r_i)e^{-2\alpha r_i}. \tag{3}$$

$V_M(i)$ is equivalent to the electrostatic potential produced by the configuration $1s^2$ in the presence of a nuclear charge α [16].

V_{ps} is a pseudopotential of the form

$$V_{ps} = MP = M[P(1) + P(2) - P(1)P(2)]. \tag{4}$$

M is an arbitrary large number, and we define the P projector as follows:

$$P(i) = |1s(i)\rangle\langle 1s(i)|, \tag{5}$$

where $1s(i)$ is the lowest eigenvalue of the Hamiltonian $H_0(i) + V_M(i)$. Note that this solution is unphysical since it violates the Pauli principle. It generates unphysical $1snl$ bound states and $1skl$ continuum states in the H spectrum. The parameter α defined in expression (3) is adjusted so that the second eigenvalue of the Hamiltonian $H_0(i) + V_M(i)$ coincides with the experimental Be$^+$($2s$) energy (with $\alpha = 2.333\,71$ we obtain $E_{\text{Be}^+(2s)} = -0.666\,54$ a.u.). The pseudopotential V_{ps} is used to eliminate the unphysical solutions of type $1snl$ (or $1skl$ continuum states) of the equation (1) [17]. The pseudopotential approach has been widely used to calculate autoionizing resonances in the Feshback formalism [18]. The diagonalization of Eq. (1) now directly gives the fundamental state Be($2s^2$). We obtain $E_{\text{Be}(2s^2)} = -1.013\,09$ a.u., a value in good agreement with the experimental value $-1.011\,85$ a.u. [20].

The solution of Eq. (1) is expanded on the basis of two-electron configurations that are products of one-electron functions as follows:

$$\Psi_n^{L,M}(\mathbf{r}_1, \mathbf{r}_2) = \mathcal{A}\sum_{\alpha \equiv i,j,l_1,l_2} c_{n,\alpha}^{L,M}\frac{B_i(r_1)}{r_1}\frac{B_j(r_2)}{r_2}\mathcal{Y}_{l_1,l_2}^{L,M}(1,2), \tag{6}$$

where $\mathcal{A}$ is the antisymmetrization operator, l_i is the angular momentum of the valence electron i, and $\mathcal{Y}_{l_1,l_2}^{L,M}(1,2)$ is a bipolar spherical harmonic. A direct diagonalization of Eq. (1) gives the eigenenergies and the expansion coefficients $c_{n,\alpha}^{L,M}$ of the bound and continuum states. We point out here that we use B-spline functions $B_i^k(r)$ to represent the radial part of the wave functions [21]. The specificity of our numerical approach is that the system is confined in a radial box whose length R_{max} is explicitly defined. Consequently the whole atomic spectrum is represented by discrete states and the density of continuum states can be controlled. This reduces considerably the numerical difficulties in both perturbative and nonperturbative approaches (see Ref. [22] for a review).

We now investigate the case of the ionization of the $1s^2$ core. As seen above, it occurs at a short wavelength, and the ionization of the valence electrons plays a minor role. We will consider that the $2s^2$ valence shell is frozen during the laser-atom interaction (this point will be discussed in the following section). The electrostatic potential created by the $2s^2$ configuration is given by

$$V_M'(i) = \frac{2}{r_i} - \frac{2}{r_i}\left(1 + \frac{3}{4}\alpha' r_i + \frac{1}{4}\alpha'^2 r_i^2 + \frac{1}{8}\alpha'^3 r_i^3\right)e^{-\alpha' r_i}, \tag{7}$$

where the hydrogenic orbital $2s$ is calculated with the effective charge α'. In order to be consistent with the calculation of the Be$^+$($2s$) state, we choose the effective charge $\alpha' = 2.309\,18$, which gives a hydrogenic energy of $-0.666\,54$ a.u., i.e., the experimental energy of Be$^+$($2s$).

B. Time-dependent calculations

Let us now consider briefly the interaction between the atom and the laser field. Within the dipole approximation, the time-dependent Schrödinger equation to be solved is given, in the length gauge, by

$$i\frac{\partial}{\partial t}\Psi(\mathbf{r}_1,\mathbf{r}_2,t) = \left[H - \sum_{i=1,2}\mathbf{E}(t)\cdot\mathbf{r}_i\right]\Psi(\mathbf{r}_1,\mathbf{r}_2,t), \qquad (8)$$

with the electric field defined as

$$\mathbf{E}(t) = -\frac{\partial}{\partial t}\mathbf{A}(t). \qquad (9)$$

The vector potential, polarized along the z axis, is defined as

$$\mathbf{A}(t) = A_0\left(\cos\frac{\pi}{T}t\right)^2\cos(\omega t)\mathbf{e}_z, \qquad (10)$$

where T is the total pulse duration, $-T/2 \leq t \leq T/2$, and ω is the photon energy. The time-dependent total wave function is expanded on the basis of the field-free atomic eigenstates, normalized to unity,

$$\Psi(\mathbf{r}_1,\mathbf{r}_2,t) = \sum_{\alpha\equiv n,L}^{N_s,L_{max}} C_\alpha(t)\Psi_n^{L,M}(\mathbf{r}_1,\mathbf{r}_2). \qquad (11)$$

Equation (8) is integrated over the total pulse duration T. The initial condition is given by

$$\Psi(\mathbf{r}_1,\mathbf{r}_2,t=-T/2) = \Psi_{in}^{L,M=0}(\mathbf{r}_1,\mathbf{r}_2), \qquad (12)$$

where $\Psi_{in}^{L,M=0}(\mathbf{r}_1,\mathbf{r}_2)$ is the initial state of the field-free system.

At the end of the pulse, the population of a given stationary state $\Psi_{klk'l'}^{LM=0}(\mathbf{r}_1,\mathbf{r}_2)$ is obtained by projecting this state on the total wave function:

$$P^L(klk'l') = |\langle\Psi_{klk'l'}^{LM=0}(\mathbf{r}_1,\mathbf{r}_2)|\Psi(\mathbf{r}_1,\mathbf{r}_2,t=T/2)\rangle|^2. \qquad (13)$$

We use a simple antisymmetrized product of orbital $\phi_{kl}(r)$ of Be$^+$ to represent the double continuum. It has been showed in paper I that this approximation, of order zero in perturbation theory, gives the leading contribution to the two-photon double ionization process.

The one-electron energy distribution in the atomic double continuum is given by

$$\frac{dP^L(kl)}{dk} = \sum_{k'l'}P^L(klk'l')\rho(kl), \qquad (14)$$

where $\rho(kl)$ is the density of states in the continuum kl.

We calculate the total-integrated cross sections by using the following expression:

$$\sigma(N\gamma,2e) = \left(\frac{\omega}{I}\right)^N\frac{P_{kk}}{C(N)T}, \qquad (15)$$

where I is the intensity in W/cm^2, ω the photon energy in joules, N the number of photons absorbed, and T the total pulse duration in seconds. Cross sections are expressed in cm^{2N} s^{N-1}. The dimensionless coefficients $C(N)$ take into
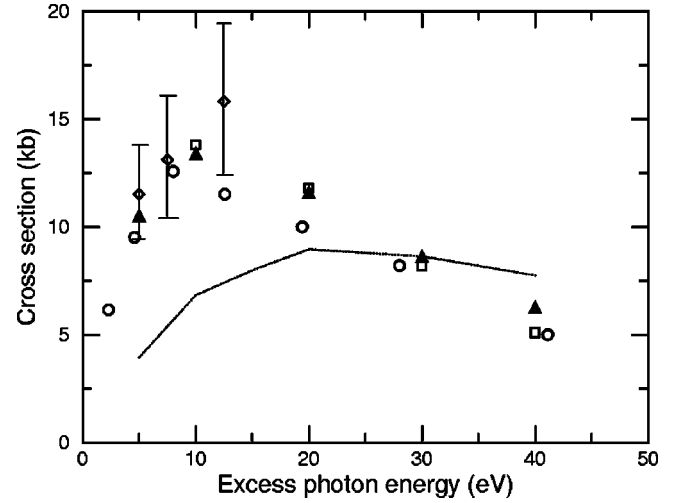

FIG. 1. The $(\gamma,2e)$ cross sections (full triangles) calculated at various excess photon energies (in eV). Empty diamonds with error bars: measurements on Be [12]. Theoretical values of Colgan and Pindzola [8] (empty squares) and Kheifets and Bray [9] (empty circles). Full curve: our calculations on He. Cross sections are expressed in kb. Results [8,9,12] are extracted from Fig. 4 in Ref. [11].

account the time dependence of the intensity, $C(1) = \frac{3}{8}$, $C(2) = \frac{35}{128}$. P_{kk} is the total probability of double ionization.

III. RESULTS AND DISCUSSION

The TDSE calculations have been performed in the length gauge and the probabilities are evaluated in the Schrödinger picture at $t=T/2$. We have checked that the results are similar in the velocity gauge and interaction picture. The cross sections have been evaluated with formula (15). Such an approach is valid as far as the total probability P_{kk} is calculated in the perturbative regime, which is the case here. The peak intensity is 10^{14} W/cm^2, and the pulse duration is given in the text.

A. Ionization of the valence electrons

Figure 1 shows the one-photon double ionization $(\gamma,2e)$ cross section versus the excess photon energy $\omega - I_p$ (I_p being the double ionization potential) given in eV. Other theoretical [8,9] and experimental [12] results are also shown in the figure. The calculations have been performed with a pulse duration of ten optical cycles. The B-spline basis sets and the configurations used in expansion (6) are given in Table I. In the case of one-photon double ionization, the total angular momentum of the final states is $L=1$, so here we have used basis II, which has more angular pairs (l_1,l_2). Our results are in good agreement with other theoretical calculations. We can observe that the various calculations available agree with the experimental measurements with error bars. In Fig. 1 we also plotted the curve corresponding to the helium cross sections. The double ionization cross sections are of the same order of magnitude in He and Be. At low excess energies, the

TABLE I. The (l_1, l_2) pairs of angular momenta and total number of combination terms N_{comb} used in Eq. (6), for each total angular momentum L and for two different B-spline basis sets, with $k=7$ and a linear knot sequence.

| Angular momentum L | Basis I ($R_{max}=50$ a.u.; $N_b=50$) | | Basis II ($R_{max}=30$ a.u.; $N_b=40$) | |
	(l_1, l_2) angular pairs	N_{comb}	(l_1, l_2) angular pairs	N_{comb}
$L=0$	(0,0) (1,1) (2,2) (3,3)	5100	(0,0) (1,1) (2,2) (3,3)	3280
$L=1$	(0,1) (1,2)	5000	(0,1) (1,2) (2,3)	4800
$L=2$	(0,2) (1,1) (1,3)	6275	(0,2) (1,1) (1,3) (2,2) (3,3)	5660

Be cross section dominates and falls for larger excess photon energies. A similar feature has been observed by Citrini *et al.* [11]. We have also checked that the one-photon single ionization cross section (γ, e) is in very good agreement with the experimental values given in Ref. [12].

In Fig. 2 we show the partial and total cross sections $(2\gamma, 2e)$ for the double ionization of beryllium through two-photon absorption, for photon energies ranging from $\omega=14$ to 20 eV. The pulse has a total duration of eight optical cycles, and we use the B-spline basis set I (see Table I). Before studying in more detail the evolution of cross sections with the photon energy, we examine the various channels leading to the double ionization processes with the absorption of two photons (see the diagram in Fig. 3). For frequencies lower than 0.52 a.u. (0.505 a.u.$<\omega<$0.52 a.u.), the double ionization process in Be is only direct; the two valence electrons are directly ejected in the double continuum. For photon frequencies larger than 0.52 a.u., the process is either direct or sequential. This latter mechanism only involves the ionization of Be$^+$(2p) for 0.52 a.u.$<\omega<$0.66 a.u. For $\omega>$0.66 a.u. (18 eV), the Be$^+$(2s) channel is open for double ionization. It is important to note that the sequential channel which does not require correlation to be populated

involves the production of Be$^+$(2s) in the intermediate step. Indeed, in contrast with the dipole coupling between $2s^2$ and $2skp$, the $2s^2$-$2pkl$ dipole coupling is zero in the zero-order perturbation theory in $1/r_{12}$. Therefore, one can surmise that the sequential process which involves the Be$^+$(2s) ion in the intermediate step will dominate for $\omega>$0.66 a.u. (this will be confirmed later). We note that there is a maximum of the cross section at 0.66 a.u. in Fig. 2. We have checked that such a maximum also exists in the helium case for a photon energy of 2 a.u. Therefore, the two-photon double ionization rate has a maximum when the sequential channel opens. This is also observed in magnesium [7]. Figure 2 shows that, as in the case of He, the D wave dominates. The contribution of the different angular channels is discussed in the following section.

Figure 4(a) shows the total electron spectrum resulting from two-photon double ionization of Be with a photon energy of 0.9 a.u. (24.5 eV). The calculations include the channels given in basis I of Table I. Three total pulse durations are considered: 14 optical cycles (about 2.36 fs), ten optical cycles (1.7 fs), and six optical cycles (1 fs). We have drawn the total density of probability $dP^L(kl)/dk$ [see Eq. (14)]. There are two well-defined peaks for the longest pulse dura-
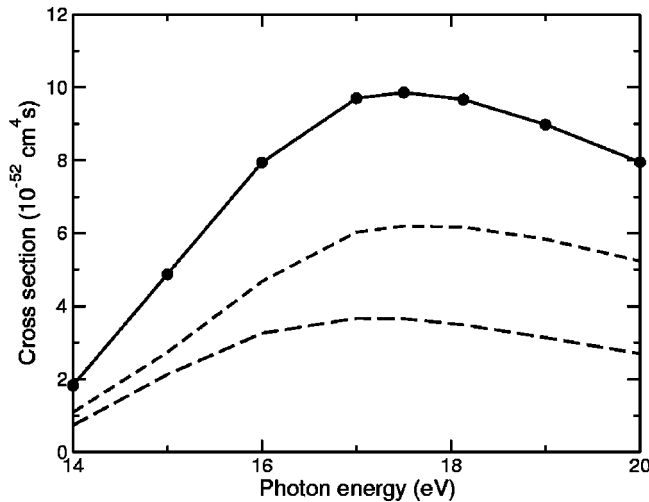

FIG. 2. The $(2\gamma, 2e)$ total cross sections (full curve) vs the photon energy (in eV). The contributions of the D wave (dashed curve) and S wave (long-dashed curve) are represented. Cross sections are expressed in cm^4 s.
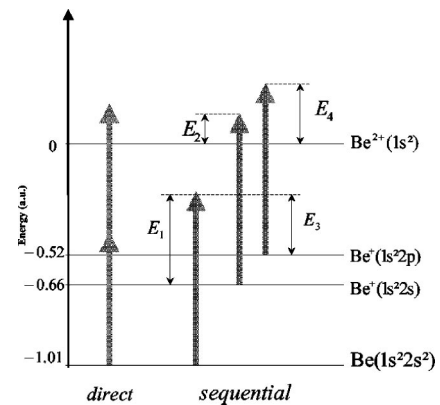

FIG. 3. Schematic Be energy level diagram, showing the direct and sequential two-photon double ionization channels from $2s^2$. In the sequential case the diagram shows the two paths to double ionize Be. The first one involves the Be$^+$(2s) ion, and the ejected electrons have the energies E_1 and E_2. In the second path, which involves Be$^+$(2p), the ejected electrons have the energies E_3 and E_4. The energies are given in a.u.

FIG. 5. The (γ, e) total cross sections for the $1s^2$ electronic core (full curve) and $2s^2$ valence electrons (dashed curve). The cross sections are expressed in Mb.
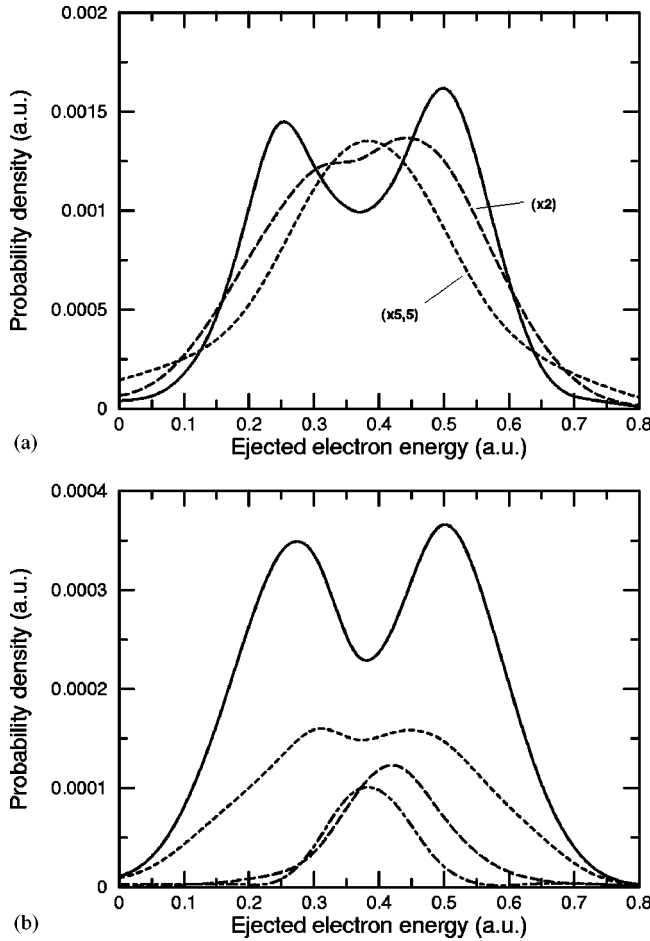

FIG. 4. (a) $(2\gamma, 2e)$ electron energy distribution spectrum for $\omega = 0.9$ a.u., $I = 10^{14}$ W/cm^2, and a total pulse duration of six (dashed curve), ten (long-dashed curve), and 14 optical cycles (full curve). (b) $(2\gamma, 2e)$ electron energy distribution spectrum in the channels $(L=2, l_1=1, l_2=1)$ (full curve), $(L=2, l_1=0, l_2=2)$ (long-dashed curve), $(L=0, l_1=1, l_2=1)$ (dashed curve), and $(L=0, l_1=2, l_2=2)$ (dotted-dashed curve), for a total pulse duration of ten optical cycles.

the intermediate channel Be($2pkl$) with $l=0$ or 2. The one-photon ionization of Be leaving the ion Be$^+$ in the $2p$ state leads to an ejected electron energy of 0.41 a.u. The ionization of the ion Be$^+(2p)$ produces an electron of energy 0.38 a.u. In fact, due to the laser bandwidth, the corresponding structures cannot be resolved and the probabilities have a maximum at about 0.4 a.u. in Fig. 4(b).

We now analyze the behavior of the energy distribution spectrum for ultrashort pulse durations. We see in Fig. 4(a) that the two peaks move towards each other for decreasing pulse durations. In the limit of the shorter pulse duration there is only one peak. This occurs when the Be$^+$ ion has no time to relax to the Be$^+(2s)$ stationary state before the second photon is absorbed. We have noticed that the electron interaction in the initial state is 0.31 a.u.. In terms of time it is 0.49 fs, which is the full width at half maximum duration of the shorter pulse in Fig. 4(a). In this latter case the distinction between direct and sequential process is not pertinent.

tion, at 0.25 and 0.50 a.u., respectively. The latter peak corresponds to the one-photon ionization of Be leaving Be$^+$ in the $2s$ state, the ejected electron having an energy of 0.55 a.u. The second peak is the signature of the ionization of the Be$^+(2s)$. The ejected electron has an energy of 0.24 a.u. The total energy in the double continuum is the photon excess energy $2\omega - I_p$. The energy difference between the peaks is the electron interaction energy in the initial state; here it is 0.31 a.u. Figure 4(a) confirms that the dominant channel for double ionization is sequential, and involves the production of the Be$^+(2s)$ ion in the intermediate step. In Fig. 4(b) we have represented the contributions of the main double ionization channels for the case of a pulse duration of ten optical cycles. The figure shows that, as expected, the main contribution to the double ionization comes from the channel $(l_1=1, l_2=1)$ that does not require correlations to be populated. There are also contributions from the channels $(l_1=0, l_2=2)$ and $(l_1=2, l_2=2)$. They are populated from the $2p^2$ component of the initial state, and the process involves
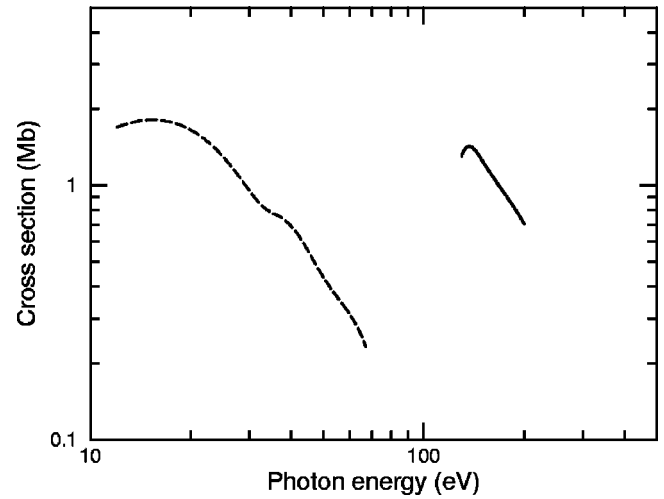
B. Towards the ionization of the electronic core

In order to complete our study of the double photoionization of beryllium, we now explore the main features of the double ionization of the $1s^2$ core of Be. In our approximation, the $2s^2$ state is frozen and represented by the model potential V'_M [see Eq. (7)]. The energy of the $1s^2$ shell of Be is calculated at -11.6 a.u. (-315.5 eV), and the ionization potential is found at 4.64 a.u. (126.2 eV). The two-photon double ionization of the $1s^2$ core requires a minimum photon energy of 157.8 eV. It is direct for 157.8 eV$< \omega <$189.4 eV and the sequential double ionization is energetically permitted for $\omega >$189.4 eV. In this calculation, the B-spline basis set is similar to the one used before, but we have scaled the box length ($R_{max}=25$ a.u.) in order to represent correctly the $1s$ orbitals in the presence of the nucleus charge $Z=4$. In Fig. 5 we show the one-photon single ionization cross sections of the $1s^2$ core and $2s^2$ valence shell of Be (the latter curve is calculated with the approach exposed in Sec. III A). As ex-
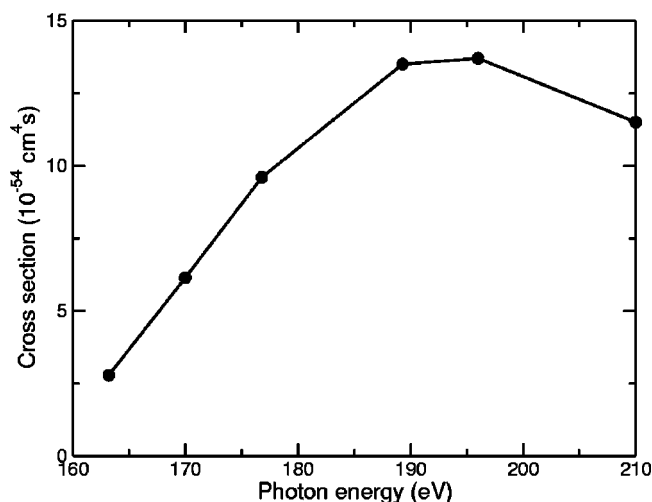
FIG. 6. The $(2\gamma, 2e)$ total cross sections for the $1s^2$ electronic core, at various photon energies (in eV). Cross sections are expressed in cm^4 s.

pected, the ionization cross section of the $1s^2$ core is much larger than the ionization of $2s^2$ for $\omega > 130$ eV. The ionization of the inner shell dominates at these photon energies. The cross sections shown in Fig. 5 are in good agreement with other recent theoretical results (see Fig. 1 in Ref. [10]).

In Fig. 6 we present the cross sections for two-photon double ionization of the core versus the photon energy. The photon energies range from 160 to 210 eV. They are calculated with a total pulse duration of ten optical cycles (i.e., $T < 1$ fs). Figure 6 shows that, as previously observed for the double ionization of $2s^2$, the cross section has a maximum at the threshold of the sequential process, i.e., at $\omega \approx 190$ eV.

It is worth noticing that the dynamics of the two-photon double ionization process will strongly depend on the pulse duration. Indeed, one-photon ionization of the core produces a nonstationary state $Be^+(1s, 2s^2)$. We assume that this ion will mainly relax to $Be^+(1s, 2lnl)$ autoionizing states which decay to the $1s^2ks$ continua. In the context of sequential double ionization, our model of the frozen $2s^2$ configuration is valid as far as $Be^+(1s, 2s^2)$ does not decay to $Be^+(1s^2, ks)$ before the second photon is absorbed. We have estimated the autoionizing lifetime of $Be^+(1s, 2s^2)$ on the basis of the resonance parameters of $Be^+(1s, 2lnl)$ [19]: it is in general of the order of 10 fs (or larger). Note that it is also the case for the $Be^{2+}(2lnl)$ resonances [19]. The conclusion is that our approach should be valid in the femto- and subfemtosecond regime, where the $2s^2$ configuration relaxes in the post laser-atom interaction channel (i.e., at $t \gg T/2$).

IV. CONCLUSION

We have studied the double ionization of Be by ultrashort laser fields by resolving the time-dependent Schrödinger equation. We have obtained cross sections for one-photon double ionization of the valence electrons, in good agree-

ment with other theoretical and experimental results. We have focused on the two-photon double ionization of the valence electrons, which occur for photon energies larger than 14 eV, the sequential channel being open for double ionization for photon energies larger than 18 eV. The associated cross section increases with the photon energy ω until $\omega \approx 18$ eV, and it decreases for higher frequencies. Therefore, the two-photon double ionization cross section is maximum in the region of the threshold for the sequential process. This feature is observed in other systems. For $\omega > 18$ eV the electron energy distribution shows two peaks separated by the electron-electron interaction in the $Be(2s^2)$ state. The peak at large energy corresponds to the one-photon ionization of $Be(2s^2)$, populating the $2skp$ channel, while the other peak, positioned at a lower energy, is associated with the one-photon ionization of $Be^+(2s)$. At short pulse durations ($T \approx 1$ fs) the Be^+ ion has no time to relax to the stationary state $Be^+(2s)$, and the two peaks move toward the same position. This feature has been already observed in helium. In the case of beryllium, less energetic photons and longer pulse durations are used. Therefore, the case of alkaline earths like Be, Mg, or Ca should be more favorable for experiments.

The case of the double ionization of the $1s^2$ core of Be has been investigated in the subfemtosecond regime. It requires intensities and photon energies which should be available in the near future with the FEL sources. Two-photon double ionization requires a minimum photon energy of 160 eV. At this energy the photoionization of the valence electrons does not play a significant role, and we represent the frozen $2s^2$ configuration with a model potential. Note that the electronic correlation time in the $1s^2$ state is close to 0.06 fs, which is shorter than the pulse duration ($T \approx 0.2$ fs). We have checked that our model gives one-photon single ionization cross sections that are in good agreement with other theoretical values. We have calculated cross sections for the double ionization of the Be core through two-photon absorption, for photon energies ranging from 160 to 210 eV. In this context, our treatment is strictly valid as far as the relaxation of the frozen configuration does not occur during the sequential double ionization process. For long pulses durations ($T \gg 1$ fs), the second ionization step should be strongly affected, and the two active electron model is not valid. These effects require further investigation.

The study of multiple electron ionization through multiphoton absorption in complex atoms is in its infancy. With femto- and subfemtosecond laser pulses the laser-atom interaction time is of the order of magnitude of the internal atomic correlation times. This opens the way to observe new dynamical effects. We have shown that alkaline earths are good candidates for experiments.

[1] J. Andruszkow *et al.*, Phys. Rev. Lett. **85**, 3825 (2000).

[2] V. Ayvazyan *et al.*, Phys. Rev. Lett. **88**, 104802 (2002).

[3] L. H. Yu, L. DiMauro, A. Doyuran, W. S. Graves, E. D. Johnson, R. Heese, S. Krinsky, H. Loos, J. B. Murphy, G. Rakowsky, J. Rose, T. Shaftan, B. Sheehy, J. Skaritka, X. J. Wang, and Z. Wu, Phys. Rev. Lett. **91**, 074801 (2003).

[4] S. Kazamias, F. Weihe, D. Douillet, C. Valentin, T. Planchon, S. Sebban, G. Grillon, F. Augé, D. Hulin, and Ph. Balcou, Eur. Phys. J. D **21**, 353 (2002).

[5] N. A. Papadogiannis, L. A. A. Nikolopoulos, D. Charalambidis, G. D. Tsakiris, P. Tzallas, and K. Witte, Phys. Rev. Lett. **90**, 133902 (2003).

[6] S. Laulan and H. Bachau, Phys. Rev. A **68**, 013409 (2003).

[7] L. A. A. Nikolopoulos, T. Nakajima, and P. Lambropoulos, Phys. Rev. Lett. **90**, 043003 (2003).

[8] J. Colgan and M. S. Pindzola, Phys. Rev. A **65**, 022709 (2002).

[9] A. S. Kheifets and I. Bray, Phys. Rev. A **65**, 012710 (2001).

[10] A. S. Kheifets and I. Bray, J. Phys. B **36**, L211 (2003).

[11] F. Citrini, L. Malegat, P. Selles and A. K. Kazansky, Phys. Rev. A **67**, 042709 (2003).

[12] R. Wehlitz and S. B. Whitfield, J. Phys. B **34**, L719 (2001).

[13] H. Bachau and P. Lambropoulos, Phys. Rev. A **44**, R9 (1991).

[14] B. Piraux, J. Bauer, S. Laulan, and H. Bachau, in Proceedings of the International Conference on Multiphoton Processes, ICOMP IX (Elounda, Crete, Greece, 2002) [Eur. Phys. J. D **26**, 7 (2003)].

[15] P. G. Burke, *Atomic Processes and Applications* (North-Holland, Amsterdam, 1976), p. 199.

[16] H. Bachau, P. Galan, and F. Martín, Phys. Rev. A **41**, 3534 (1990).

[17] A. Martín, O. Mó, A. Riera, and M. Yáñez, Europhys. Lett. **4**, 799 (1987).

[18] H. Bachau, P. Galan, F. Martín, A. Riera, and M. Yáñez, At. Data Nucl. Data Tables **48**, 167 (1991).

[19] L. A. Vainshtein and U. I. Safronova, At. Data Nucl. Data Tables **21**, 49 (1978).

[20] S. Bashkin and J. O. Stoner, *Atomic Energy Levels and Grotian Diagrams* (North-Holland, Amsterdam, 1975), Vol. 1.

[21] C. De Boor, *A Practical Guide to Splines* (Springer, New York, 1978).

[22] H. Bachau, E. Cormier, P. Decleva, J. E. Hansen, and F. Martín, Rep. Prog. Phys. **64**, 1815 (2001).